Baseline Drift Estimation for Time Series Data Using Quantile Trend Filtering

Halley Brantley* Joseph Guinness† and Eric C. Chi‡

Abstract

We address the problem of estimating smoothly varying baseline trends in time series data using quantile trend filtering. We extend the basic framework to ensure non-crossing while estimating multiple trends simultaneously and implement an alternating direction method of moments (ADMM) algorithm for series that cannot be processed simultaneously. Timing experiments demonstrate the usefulness of our ADMM algorithm even in cases where the series can be processed simultaneously. We also address smoothing parameter selection and propose a modified criteria based on the extended Bayesian Information Criteria. We demonstrate both through simulation studies and an application to lost-cost air quality sensor data that our model provides better or comparable estimates than existing methods of non-parametric quantile trends and improves signal classification of low-cost air quality sensor output.

Keywords: quantile regression, non-parametric regression, trend estimation, smoothing splines

*Department of Statistics, North Carolina State University, Raleigh, NC 27695 (E-mail: hlbrantl@ncsu.edu)

†Department of Biological Statistics and Computational Biology, Cornell University, Ithaca, NY 14853 (E-mail: guinness@cornell.edu)

‡Department of Statistics, North Carolina State University, Raleigh, NC 27695 (E-mail: eric_chi@ncsu.edu).

1 Introduction

In applications spanning the fields of chemistry (Ning et al., 2014), macroeconomics (Yamada, 2017), environmental science (Brantley et al., 2014), and medical sciences (Pettersson et al., 2013; Marandi and Sabzpoushan, 2015), scalar time series are observed and assumed to consist of a slowly varying trend and other more rapidly varying components. Kim et al. (2009) addressed the case when the series consisted of just a trend and a random noise component and proposed the use of ℓ_1-*trend filtering* to estimate trends that piecewise linear or piecewise polynomial. Tibshirani (2014) later demonstrated that empirically the trend filtering estimates adapt to the local level of smoothness better than the more common smoothing splines **@Halley from Eric: If he proved theorems, minimax stuff, we should state that.**. In the trend filtering problem, given observations $y(t)$ with $t = 1, \ldots, n$, the trend, $\theta(t)$, is estimated by solving the following convex optimization problem. **@Halley from Eric: We maybe should define two objects $y(t)$ which is a function over the reals and $\mathbf{y} \in \mathbb{R}^n$, where $y_i = y(t_i)$.**

$$\underset{\boldsymbol{\theta}}{\text{minimize}} \; \frac{1}{2}\|\mathbf{y} - \boldsymbol{\theta}\|_2^2 + \lambda \|\mathbf{D}^{(k+1)}\boldsymbol{\theta}\|_1,$$

where $\lambda \geq 0$ is a regularization parameter and the matrix $\mathbf{D}^{(k+1)} \in \mathbb{R}^{(n-k-1)\times n}$ is the discrete difference operator of order $k+1$. To understand the purpose of penalizing $\mathbf{D}^{(k+1)}\boldsymbol{\theta}$ consider the difference operator when $k = 0$.

$$\mathbf{D}^{(1)} \;=\; \begin{pmatrix} -1 & 1 & 0 & \cdots & 0 & 0 \\ 0 & -1 & 1 & \cdots & 0 & 0 \\ \vdots & & & & & \\ 0 & 0 & 0 & \cdots & -1 & 1 \end{pmatrix}.$$

Thus, $\|\mathbf{D}^{(1)}\boldsymbol{\theta}\|_1 = \sum_{i=1}^{n-1} |\theta_i - \theta_{i+1}|$ which is just total variation denoising in one dimension. The penalty term incentivizes solutions which are piece-wise constant. For $k \geq 1$, the difference operator $\mathbf{D}^{(k+1)} \in \mathbb{R}^{(n-k-1)\times n}$ is defined recursively as follows

$$\mathbf{D}^{(k+1)} \;=\; \mathbf{D}^{(1)}\mathbf{D}^{(k)}.$$

By penalizing the $k+1$ fold composition of the discrete difference operator, we obtain solutions which are piecewise polynomials of order k.

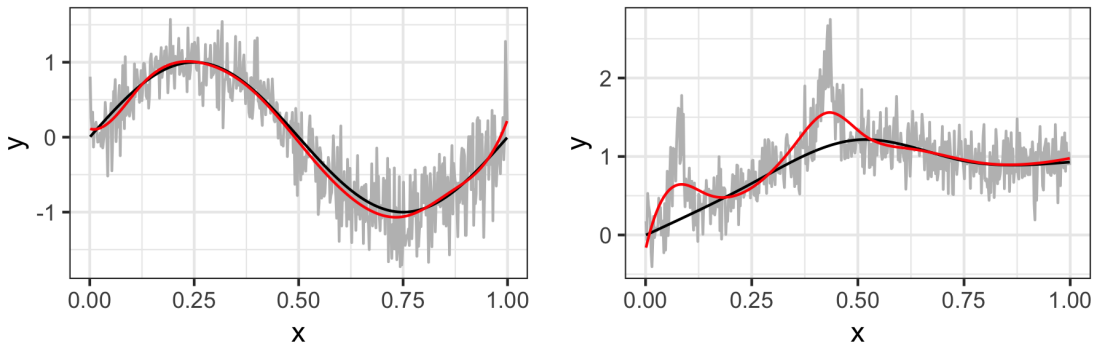

(a) Slow Trend + Noise

(b) Slow Trend + Spikes + Noise

Figure 1: Two examples of trend filtering solutions. The true trend is shown in black, while the estimated trend is shown in red. **@Halley from Eric: Could you explain to the reader what they should be seeing in the two panels, especially the one on the right? Don't leave to chance that a busy reviewer may miss the point.**

Figure 1a shows that trend filtering provides excellent estimates of trends when the only components of the time series are the trend and random noise. In some applications, however, time series may also include, in addition to the trend and noise, a signal component that varies more rapidly than the trend. Figure 1b shows that in these cases the trend filtering estimate over-estimates the trend in the places where signal is present.

One application in which the observed time series consists of a slowly varying baseline, non-negative signal, and rapidly varying noise is the output of lost-cost air quality sensors. The use of low-cost, portable, air quality sensors has increased dramatically in the last decade. These sensors can provide an un-calibrated measure of a variety of pollutants in near real time, but deriving meaningful information from sensor data remains a challenge (Snyder et al., 2013). The "SPod" is a low-cost sensor currently being investigated by researchers at the U.S. Environmental Protection Agency to detect volatile organic compound (VOC) emissions from industrial facilities (Thoma et al., 2016). To reduce cost and power consumption of the SPod, the temperature and relative humidity of the air presented to the photoionization detectors (PIDs) is not controlled and as a result the output signal exhibits a slowly varying baseline drift on the order of minutes to hours. Figure 2 provides

an example of 3 co-located SPod sensor outputs from near an industrial facility. While all of the sensors response to the pollutant signal, the amount of baseline drift varies from one node to another.

In this application, as well as those described in Ning et al. (2014), Marandi and Sabzpoushan (2015), and Pettersson et al. (2013), it is not the mean trend that is desired but rather the baseline trend, which can be thought of as a trend in a low quantile of the data. Koenker and Bassett (1978) were the first to propose substituting the squared loss typically used in regression with the check-loss function (1) to estimate a conditional quantile instead of the conditional mean.

$$\rho_\tau(\mathbf{z}) \quad = \quad \sum_{i=1}^{n} z_i(1 - \mathbb{1}(z_i < 0)), \tag{1}$$

where $\mathbb{1}(A)$ is 1 if its input A is true and 0 otherwise.

Later, Koenker et al. (1994) addressed the issue of estimated quantile curves by combining the check-loss penalty with trend filtering penalty with $k = 2$ which produces quantile trends that are piecewise linear. Other approaches to estimating quantile trends have also been proposed. Rather than using the trend filtering ℓ_1-norm to penalize the discrete differences, Nychka et al. (1995) used the smoothing spline penalty based on the ℓ_2-norm solving the optimization problem in (1).

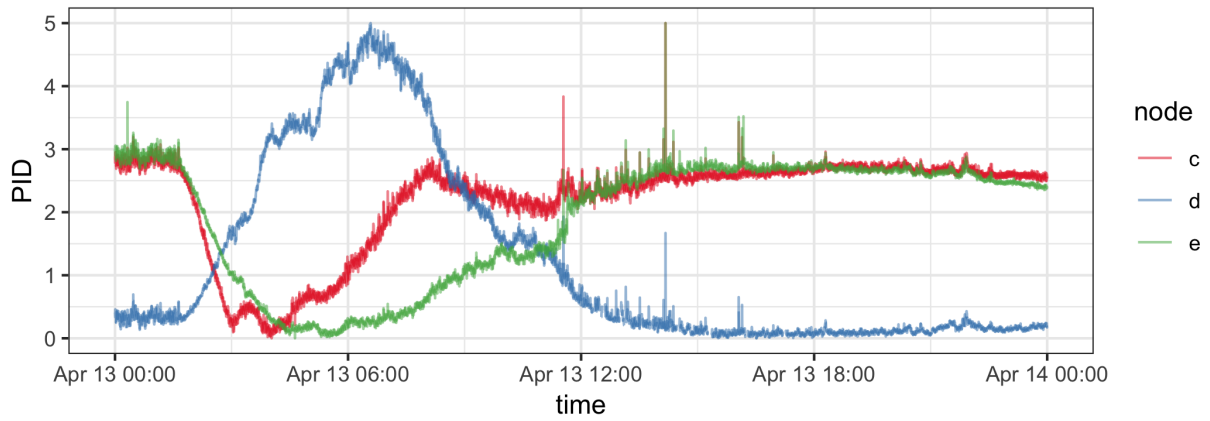

Figure 2: Example of 3 co-located SPod PID sensor readings.

$$\rho_\tau(y - f) + \lambda \int (f''(t))^2 dt,$$

where $f(t)$ is a smooth function of time and λ is a tuning parameter that controls the degrees of smoothing. **@Halley from Eric: What is $\rho_\tau(\cdot)$ when its input is a function over the reals? It's defined above as a function of a vector input.** Oh et al. (2011) proposed an algorithm for solving this problem based on approximating the check-loss function with a similar differentiable function.

Racine and Li (2017) take an entirely different approach to estimating quantile trends. They constrain the response to follow a smooth location scale model of the form $y(t) = a(t) + b(t)\epsilon_i$ and estimate the τ_{th} conditional quantile given $t = t_0$ using a kernel estimator and local linear approach.

We propose to use the trend filtering penalty combined with the check-loss function to produce quantile trends that are piecewise quadratic. The formulation was proposed by Kim et al. (2009) as a possible extension of ℓ_1-trend filtering but not studied. Moreover, we extend the basic framework to ensure non-crossing while modeling multiple quantiles. We also implement a parallel ADMM algorithm for series that are too large to be computed simultaneously and propose a modified criteria for choosing the smoothing parameter. We demonstrate through simulation studies that our proposed model provides better or comparable estimates of non-parametric quantile trends than existing methods and is a more effective method of drift removal for low-cost air quality sensors.

2 Methods

2.1 Quantile Trend Filtering

We combine the ideas of quantile regression and trend filtering. For a single quantile level τ the estimation of the quantile trend filtering model can be posed as the following convex optimization problem.

$$\underset{\boldsymbol{\theta}}{\text{minimize}}\ \rho_\tau(\mathbf{y} - \boldsymbol{\theta}) + \lambda \|\mathbf{D}^{(k+1)}\boldsymbol{\theta}\|_1, \tag{2}$$

where λ is a non-negative regularization parameter. We address the problem of choosing λ in Section 2.3. As with classic quantile regression, the quantile trend filtering problem is a linear program which can be solved by a number of free or commercial solvers. In many cases, including ours, we are interested in estimating multiple quantiles simultaneously. We also want to ensure that our quantile estimates are valid by enforcing the constraint that if $\tau_2 > \tau_1$ then $Q(\tau_2) \geq Q(\tau_1)$. **@Halley from Eric: Please define Q. The reader can infer what it is, but it's better not to put that on the reader.** Given quantiles $\{\tau_1, \ldots, \tau_J\}$ such that $\tau_1 < \tau_2 < \ldots < \tau_J$, the optimization problem becomes

$$\begin{aligned} \underset{\boldsymbol{\theta}_1,\ldots,\boldsymbol{\theta}_J}{\text{minimize}} \; & \sum_{j=1}^{J} \left[\rho_{\tau_j}(\mathbf{y} - \boldsymbol{\theta}_j) + \lambda_j \|\mathbf{D}^{(k+1)}\boldsymbol{\theta}_j\|_1 \right] \\ \text{subject to:} \; & \theta_1(t) \leq \theta_2(t) \leq \ldots \leq \theta_J(t) \text{ for all } t, \end{aligned} \tag{3}$$

where $\boldsymbol{\theta}_j \in \mathbb{R}^n$. The additional constraints are linear in the parameters so the non-crossing quantile trends can still be estimated by a number of available solvers. In the rest of this paper we rely on the commercial solver Gurobi (Gurobi Optimization, 2018) and its R package implementation, but it can easily be substituted for a free solver such as the Rglpk package by Theussl and Hornik (2017). The number of parameters to be estimated in this problem is equal to the product of the number of observations n and the number of quantiles of interest J. As the size of the data and the number of quantiles grows, all solvers will eventually break. **@Halley from Eric: Can we be more specific about what we mean when we say "break?"**

2.2 ADMM for Big Data

To our knowledge, no one has addressed the problem of finding smooth quantile trends of series that are too large to be processed simultaneously. We propose an alternating direction method of multipliers (ADMM) algorithm for solving large problems in a piecewise fashion. The ADMM algorithm (Gabay and Mercier, 1975; Glowinski and Marroco, 1975) is fully described by Boyd et al. (2011). We apply the consensus ADMM algorithm to the the quantile regression trend filtering problem given in (2), by dividing our observed series $y(t)$

with $t = \{1, \ldots, n\}$ into overlapping windows

$$
\begin{aligned}
y_1(t) &= y(t) \quad \text{if} \quad 1 \leq t \leq u_1 \\
y_2(t) &= y(t) \quad \text{if} \quad l_2 \leq t \leq u_2 \\
&\vdots \\
y_M(t) &= y(t) \quad \text{if} \quad l_M \leq t \leq n,
\end{aligned}
$$

with boundaries $1 < l_2 < u_1 < l_3 < u_2 < l_4 < u_3 < \cdots < n$. An illustration is given in Figure 3. Given quantiles $\tau_1 < \ldots < \tau_J$ to be estimated we define $\theta_{j,m}(t)$ as the value of the $\tau_j{}^{\text{th}}$ quantile trend in window M at time point t. In order to write out the constraint that the overlapping sections must be equal, we define a consensus variable

$$
\begin{aligned}
\bar{\theta}_{j,m} =& g(\theta_{j,m-1}, \theta_{j,m}, \theta_{j,m+1}) \\
=& \begin{cases}
\frac{\theta_{j,m-1}(t)+\theta_{j,m}(t)}{2} & \text{if} \quad l_m \leq t \leq u_{m-1} \\
\theta_{j,m}(t) & \text{if} \quad u_{m-1} \leq t \leq l_{m+1} \\
\frac{\theta_{j,m}(t)+\theta_{j,m+1}(t)}{2} & \text{if} \quad l_{m+1} \leq t \leq u_m
\end{cases},
\end{aligned}
$$

defining $\theta_{j,M+1} = \theta_{j,M}$ and $\theta_{j,0} = \theta_{j,1}$. Our windowed quantile trend optimization problem can then be written as

$$
\min_{\theta_{1,m},\ldots,\theta_{J,m}} \sum_{m=1}^{M} \sum_{j=1}^{J} \left[\rho_{\tau_j}(y_m - \theta_{j,m}) + \lambda_j \|\mathbf{D}^{(k+1)} \theta_{j,m}\|_1 \right]
$$

subject to:

$$
\begin{aligned}
&\theta_{1,m}(t) \leq \theta_{2,m}(t) \leq \ldots \leq \theta_{J,m}(t) \text{ for all } m, t \\
&\theta_{j,m}(t) = \bar{\theta}_{j,m}(t) \text{ for all } j, m, t
\end{aligned}
$$

Defining Lagrange multipliers $\omega_{j,m}$, and penalty parameter $\gamma > 0$ we can write the augmented Lagrangian for finding the trends in window m:

$$
\mathcal{L}(\theta_{j,m}, \bar{\theta}_{j,m}, \omega_{j,m}) = \sum_{j=1}^{J} \rho_{\tau_j}(y_m - \theta_{j,m}) + \lambda \|\mathbf{D}^{(k+1)} \theta_{j,m}\|_1 + \omega_{j,m}^{\mathsf{T}}(\theta_{j,m} - \bar{\theta}_{j,m}) + \frac{\gamma}{2} ||\theta_{j,m} - \bar{\theta}_{j,m}||_2^2
$$

Figure 3: Window boundaries and trends fit separately in each window.

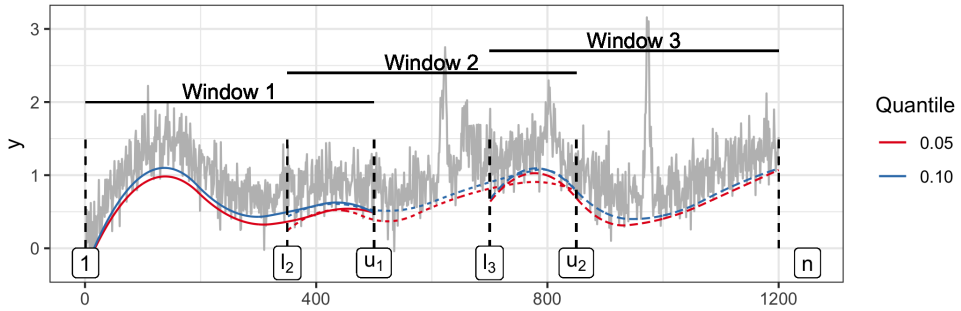

Algorithm 1 ADMM algorithm for quantile trend filtering with windows

Define $\mathbf{D} = \mathbf{D}^{(k+1)}$.

initialize:

$\boldsymbol{\theta}_{j,m}^{(0)} \leftarrow \arg\min \sum_{j=1}^{J} \rho_{\tau_j}(\mathbf{y}_m - \boldsymbol{\theta}_{j,m}) + \lambda \|\mathbf{D}\boldsymbol{\theta}_{j,m}\|_1$ subject to $\theta_{1,m}(t) < \ldots < \theta_{J,m}(t)$ for all t.

$\boldsymbol{\omega}_{j,m}^{(0)} \leftarrow \mathbf{0}$

repeat

$\bar{\theta}_{j,m}^{(q)} \leftarrow g(\theta_{j,m-1}^{(q-1)}, \theta_{j,m}^{(q-1)}, \theta_{j,m+1}^{(q-1)})$

$\omega_{j,m}^{(q)} \leftarrow \omega_{j,m}^{(q-1)} + \gamma(\theta_{j,m}^{(q-1)} - \bar{\theta}_{j,m}^{(q)})$

$\theta_{j,m}^{(q)} \leftarrow \arg\min \mathcal{L}(\theta_{j,m}, \bar{\theta}_{j,m}^{(q-1)}, \omega_{j,m}^{(q-1)})$ subject to $\theta_{1,m}(t) < \ldots < \theta_{J,m}(t)$ for all t.

until convergence

return Non-overlapping sequence of $\bar{\theta}_{j,m}^{(q)}$ for all j, m.

We then estimate the trend separately in each window, which can be done in parallel, while constraining the overlapping pieces of the trends to be equal as outlined in algorithm 1.

We measure convergence use the stopping criteria described by Boyd et al. (2011). The criteria are based on the primal and dual residuals which represent the residuals for the primal and dual feasibility, respectively. The primal residual,

$$r_p^{(q)} = \sqrt{\sum_{m=1}^{M}\sum_{j=1}^{J} \|\theta_{j,m}^{(q)} - \bar{\theta}_{j,m}^{(q)}\|_2^2},$$

represents the difference between the trend values in the windows and the consensus trend

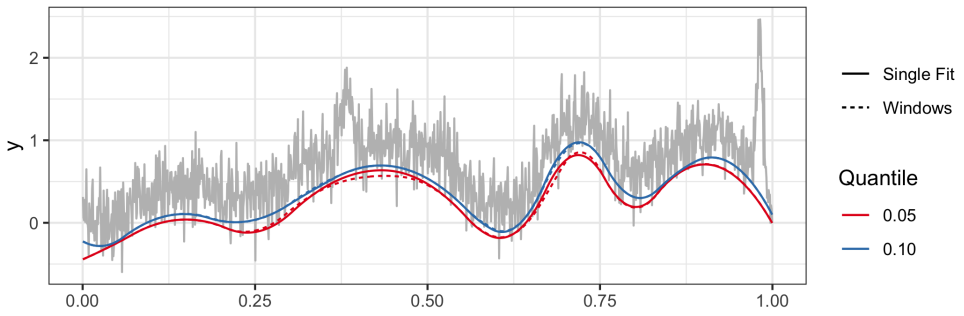

Figure 4: Trend fit with our ADMM algorithm with 3 windows which converged in 7 iterations compared to trend from simultaneous fit.

value while the dual residual,

$$r_d^{(q)} = \gamma \sqrt{\sum_{m=1}^{M} \sum_{j=1}^{J} \|\bar{\theta}_{j,m}^{(q)} - \bar{\theta}_{j,m}^{(q-1)}\|_2^2},$$

represents the change in the consensus variable from one iterate to the next. The algorithm is stopped when

$$r_p^{(q)} < \epsilon_{\text{abs}} \sqrt{nJ} + \epsilon_{\text{rel}} \max_m \left[\max \left(\sqrt{\sum_{j=1}^{J} \|\theta_{j,m}^{(q)}\|_2^2}, \sqrt{\sum_{j=1}^{J} \|\bar{\theta}_{j,m}^{(q)}\|_2^2} \right) \right]$$

$$r_d^{(q)} < \epsilon_{\text{abs}} \sqrt{nJ} + \epsilon_{\text{rel}} \sqrt{\sum_{m=1}^{M} \sum_{j=1}^{J} \|\omega_{j,m}^{(q)}\|_2^2}$$

Timing experiments illustrate the advantages of using our ADMM algorithm even on datasets where solving the problem simultaneously is possible. For each data size, n, 25 datasets were simulated using the peaks simulation design described below and trends for three quantiles were fit simultaneously: 0.05, 0.1, and 0.15 using a $\lambda = n/5$. We use from one to four windows for each data size with an overlap of 500. The windows algorithm was run until the stopping criteria were met using $\epsilon_{\text{abs}} = 0.01$ and $\epsilon_{\text{rel}} = 0.001$. Figure 5 shows that using 4 windows instead of one on data sizes of 55000 provides a factor of 3 decrease in computation time. The timing experiments were conducted on

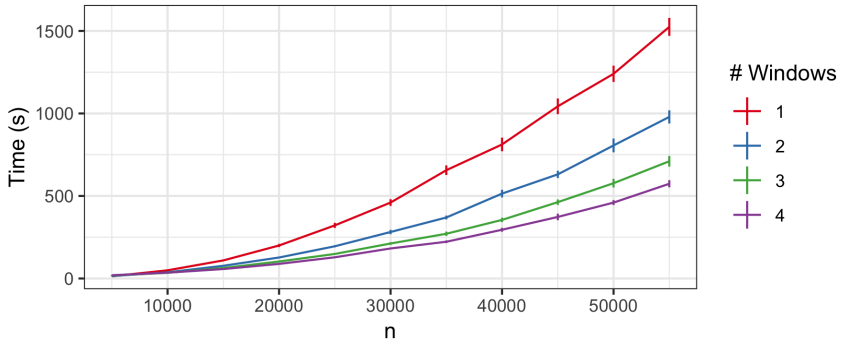

Figure 5: Timing experiments comparing quantile trend filtering with varying numbers of windows by data size.

2.3 Regularization Parameter Choice

An important problem in trend estimation is the choice of regularization parameter or degree of smoothness. Our method can easily handle missing data by defining the check-loss function to output 0 for missing values. This allows us to leave out validation observations that can be used to select the tuning parameter λ. However, the use of an information criteria metric can result in a better choice of regularization parameter than the validation method. Koenker et al. (1994) addressed the choice of regularization parameter by proposing the Schwarz criterion for the selection of λ

$$\text{SIC}(p_\lambda) \quad = \quad \log\left[\frac{1}{n}\rho_\tau(y-\theta)\right] + \frac{1}{2n}p_\lambda \log n.$$

where $p_\lambda = \sum_t \mathbb{1}(y(t) = \widehat{\theta}(t))$ is the number of interpolated points, which can be thought of as active knots. The SIC is based on the traditional Bayesian Information Criterion (BIC) which is given by

$$\text{BIC}(s) \quad = \quad -2\log(L\{\hat{\theta}\}) + \nu \log n$$

where L is the likelihood function and ν is the number of non-zero components in $\hat{\theta}$. If we take the approach used in Bayesian quantile regression (Yu and Moyeed, 2001), and assume that minimizing the check-loss function corresponds to maximizing the asymmetric Laplace likelihood,

$$L(y \mid \theta) \quad = \quad \left(\frac{\tau^n(1-\tau)}{\sigma}\right)^n \exp\left\{-\sum_t \rho_\tau\left(\frac{y(t)-\theta(t)}{\sigma}\right)\right\},$$

we can compute the BIC as

$$\text{BIC}(\text{df}) \quad = \quad 2\frac{1}{\sigma}\rho_\tau(y-\hat{\theta}) + \text{df}\log n$$

where *df* is the number of non-zero elements of $\mathbf{D}^{(k+1)}\hat{\boldsymbol{\theta}}$. We can choose any $\sigma > 0$ and have found empirically that $\sigma = \frac{1-|1-2\tau|}{2}$ produces stable estimates.

Another criteria, the extended Bayesian Information Criteria (eBIC), specifically designed for large parameter spaces was proposed by Chen and Chen (2008).

$$\text{eBIC}_\gamma(s) \quad = \quad -2\log(L\{\hat{\theta}\}) + \nu\log n + 2\gamma\log\binom{P}{\nu}, \quad \gamma \in [0,1]$$

where P is the total number of possible parameters and ν is the number of non-zero parameters included in given model. We used this criteria with $\gamma = 1$, and $P = n - k - 1$. We use a single dataset from our simulation study to illustrate the difference between the scaled, unscaled ($\sigma = 1$) and scaled extended BIC criteria in Figure 6.

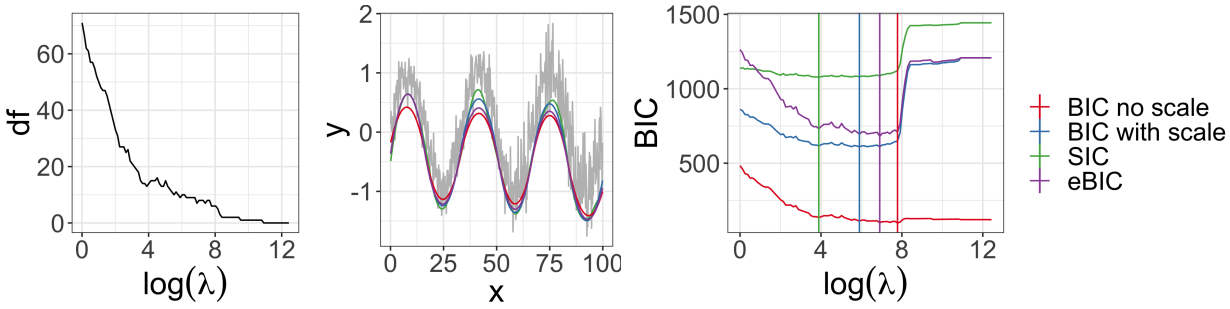

Figure 6: (Left) Degrees of freedom (number of non-zero elements of $D\theta$) by $\log(\lambda)$. (Middle) Estimated 10th quantile trend with regularization parameter chosen using various criterion. (Right) Criterion values by $\log(\lambda)$ vertical lines indicate locations of minima.

3 Simulation Studies

We conduct two simulation studies to compare the performance of our quantile trend filtering method and regularization parameter selection criteria with previously published methods. The first study compares the method's ability to estimate quantiles when the only components of the observed series are a smooth trend and a random component. The

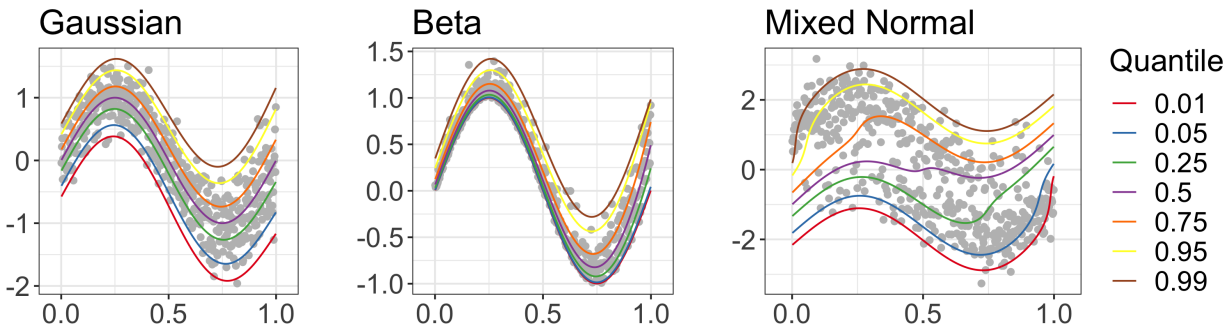

Figure 7: Simulated data with true quantile trends.

second study is based on our application and compares the method's ability to estimate baseline trends and enable peak detection when the time series contains a non-negative signal component in addition to the trend and random component.

We compare the performance of our quantile trend filtering method with three previously published methods: `npqw` which is the quantile-ll method described in Racine and Li (2017), code was obtained from the author; `qsreg` in the `fields` R package and described in Oh et al. (2011); Nychka et al. (1995); `rqss` available in the `quantreg` package and described in Koenker et al. (1994). The regularization parameter λ for the `rqss` method is chosen using a grid search and minimizing the SIC criteria as described in Koenker et al. (1994), the regularization parameter for `qsreg` was chosen using generalized cross-validation based on the quantile criterion Oh et al. (2011).

We also compare three criteria for choosing the smoothing parameter with our quantile trend filtering method with a single window: `detrendr_SIC` λ chosen using SIC (4)(Koenker et al., 1994); `detrendr_valid`: λ is chosen by leaving out every 5th observation as a validation data set and minimizing the check-loss function evaluated at the validation data; `detrendr_eBIC`: the proposed scaled eBIC criteria (4).

3.1 Estimating Quantiles

To compare performance in estimating quantile trends, three simulation designs from Racine and Li (2017) were considered. For all designs $t = 1, \ldots, n$, $x(t) = t/n$, and

the response y was generated as

$$y(t) = sin(2\pi x(t)) + \epsilon(x(t))$$

The three error distributions considered were

- Gaussian: $\epsilon(x(t)) \sim N\left(0, \left(\frac{1+x(t)^2}{4}\right)^2\right)$
- Beta: $\epsilon(x(t)) \sim Beta(1, 11 - 10x(t))$
- Mixed normal: $\epsilon(x(t))$ is simulated from a mixture of $N(-1, 1)$ and $N(1, 1)$ with mixing probability $x(t)$.

One hundred datasets were generated of sizes 300, 500 and 1000. For each method quantile trends were estimated for $\tau = \{0.05, 0.25, 0.5, 0.75, 0.95\}$. Only our detrend methods guarantee non-crossing quantiles. For each quantile trend and method the root mean squared error was calculated as RMSE $= \sqrt{\frac{1}{n}\sum_t (\hat{q}_\tau(t) - q_\tau(t))^2}$. The mean RMSE $\pm$ twice the standard error for each method, quantile level and sample size is shown in Figure 8. In all three designs the proposed detrend methods are either better than or comparable to existing methods. Overall the `detrend_eBIC` performs best, and especially in the mixed normal design our methods have lower RMSEs for the 5^{th} and 95_{th} quantiles. The `npqw` method performs particularly poorly in the mixed normal design due to the fact that it assumes the data comes from a scale-location model which is violated in this case.

3.2 Peak Detection

We use another simulation design based on the applied problem we aim to solve. We assume that the measured data can be represented by

$$Y(t) \quad = \quad s(t) + b(t) + \epsilon(t)$$

with $t = 1, \ldots, n$, where $s(t)$ is the true signal at time t, $b(t)$ is the drift component that varies smoothly over time and $\epsilon(t) \sim N(0, 0.25^2)$ is an error component. We generate $b(t)$ using cubic natural spline basis functions with degrees of freedom sampled from a Poisson distribution with mean parameter equal to $n/100$, and coefficients drawn from an

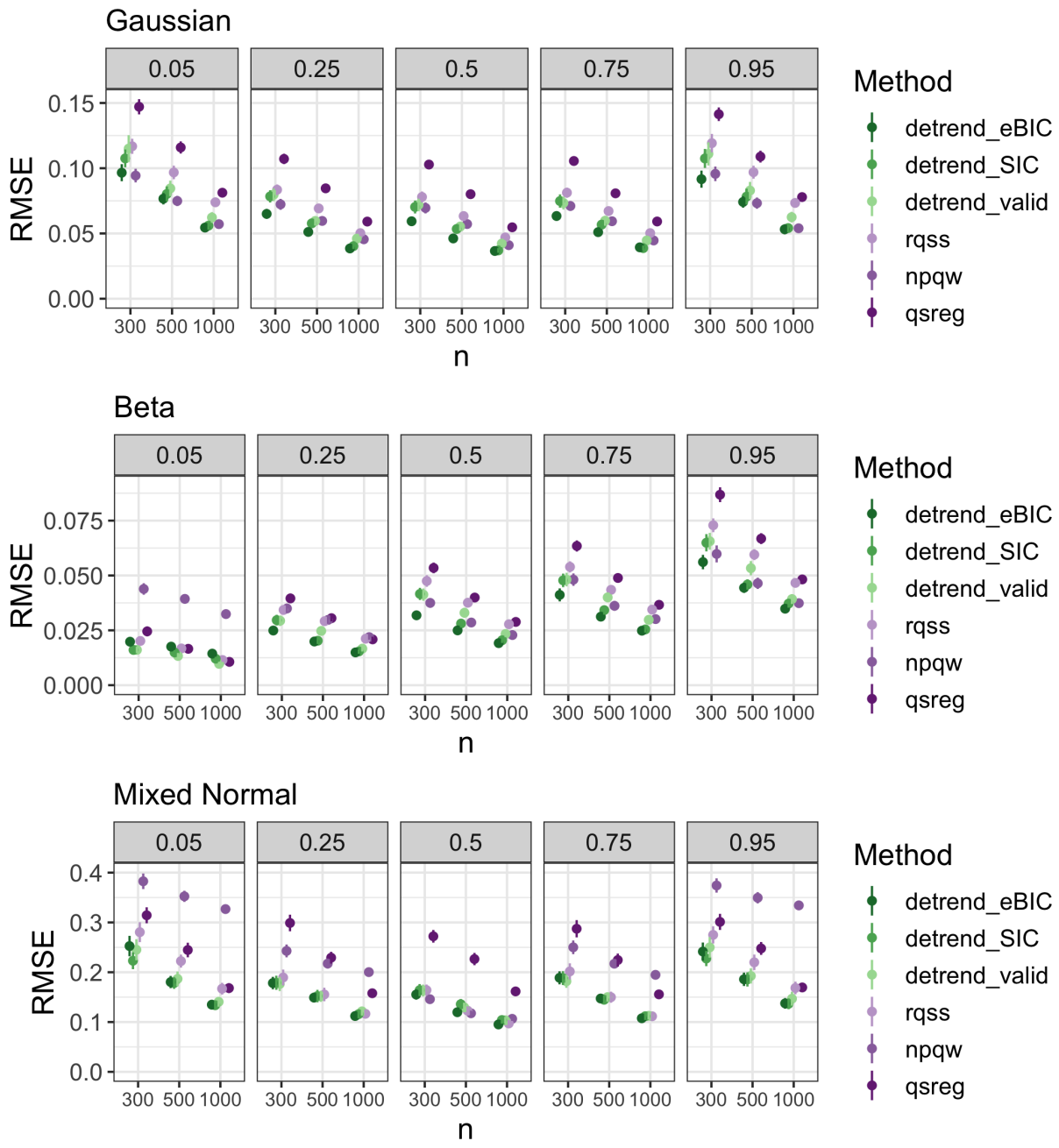

Figure 8: RMSE by design, method, quantile and data size. Points and error bars represent mean RMSE ± twice the standard error.

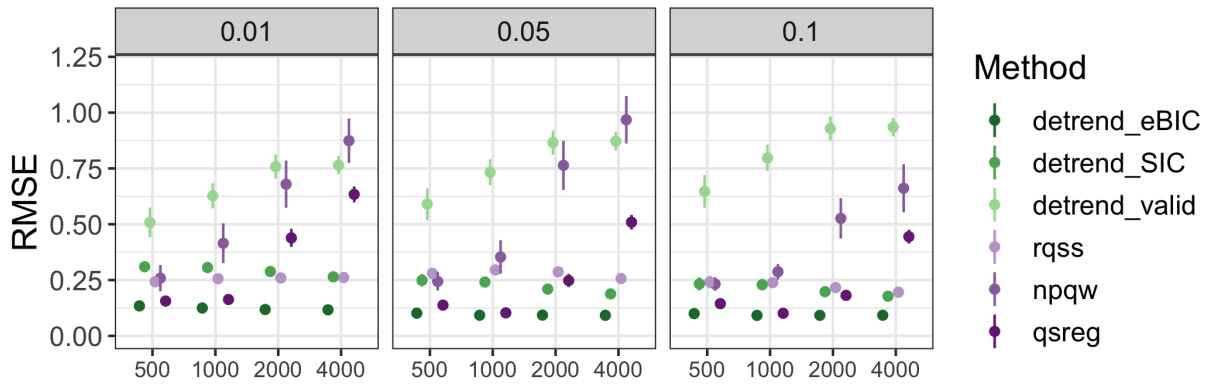

Figure 9: RMSE by method, quantile and data size for peaks design.

exponential distribution with rate 1. The true signal function is assumed to be zero with peaks generated using the Gaussian density function. The number of peaks is sampled from a binomial distribution with size equal to n and probability equal to 0.005 with location parameters uniformly distributed between 1 and $n-1$ and bandwidths uniformly distributed between 2 and 12. The simulated peaks were multiplied by a factor that was randomly drawn from a normal distribution with mean 20 and standard deviation of 4. One hundred datasets were generated for each $n = \{500, 1000, 2000, 4000\}$. We compare the ability of the methods to estimate the true quantiles of $Y(t) - s(t)$ for $\tau \in \{0.01, 0.05, 0.1\}$ and calculate the RMSE (Figure 9). In this simulation study our `detrend_eBIC` method outperforms the others substantially. The `qsreg` method is comparable to the `detrend_eBIC` method on the smaller datasets but its performance deteriorates as the data size grows. The `npqw` and `detrend_valid` methods both perform poorly on this design.

In our application, we want to accurately classify the observations into signal and no signal using a threshold. To evaluate the accuracy of our method compared to other methods we define true signal as any time point when the simulated peak value is greater than 0.5. We compare three different quantiles for the baseline estimation and four different thresholds for classifying the signal after subtracting the estimated baseline from the observations. An illustration of the observations classified as signal after subtracting the baseline trend compared to the "true signal" is shown in Figure 10. To compare the resulting signal classifications we calculate the class averaged accuracy (CAA). Defining $s(t) \in \{0, 1\}$ as the

vector of true signal classification and $\hat{s}(t) \in \{0, 1\}$ as the estimated signal classification, the CAA is defined as

$$\text{CAA} \quad = \quad \frac{1}{2}\left(\frac{\sum_{t=1}^{n} \mathbb{1}[s(t) = 1 \cap \hat{s}(t) = 1]}{\sum_{t=1}^{n} \mathbb{1}[s(t) = 1]} + \frac{\sum_{t=1}^{n} \mathbb{1}[s(t) = 0 \cap \hat{s}(t) = 0]}{\sum_{t=1}^{n} \mathbb{1}[s(t) = 0]}\right).$$

We use this metric because our classes tend to be very un-balanced with many more 0s than 1s. The CAA metric will always give a score of 0.5 for random guessing and also for trivial classifiers such as $\hat{s}(t) = 0$ for all t.

Our `detrend_BIC` method performs the best overall in terms of both RMSE and CAA. While `qsreg` was competitive with our method in some cases, in the majority of cases the largest CAA values for each threshold were produced using the `detrend_eBIC` method with the 1^{st} or 5^{th} quantiles.

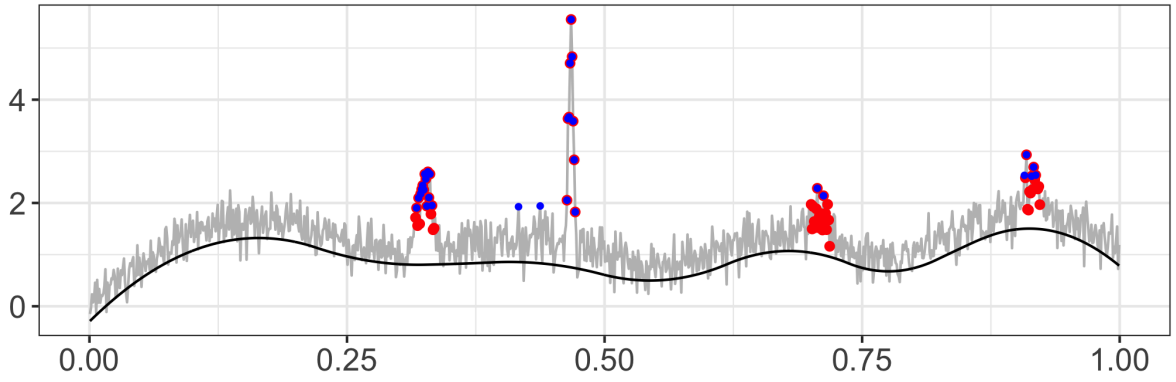

Figure 10: Example signal classification using threshold. Red indicates true signal > 0.5, blue indicates observations classified as signal after baseline removal using `detrend_eBIC` and a threshold of 1.2.

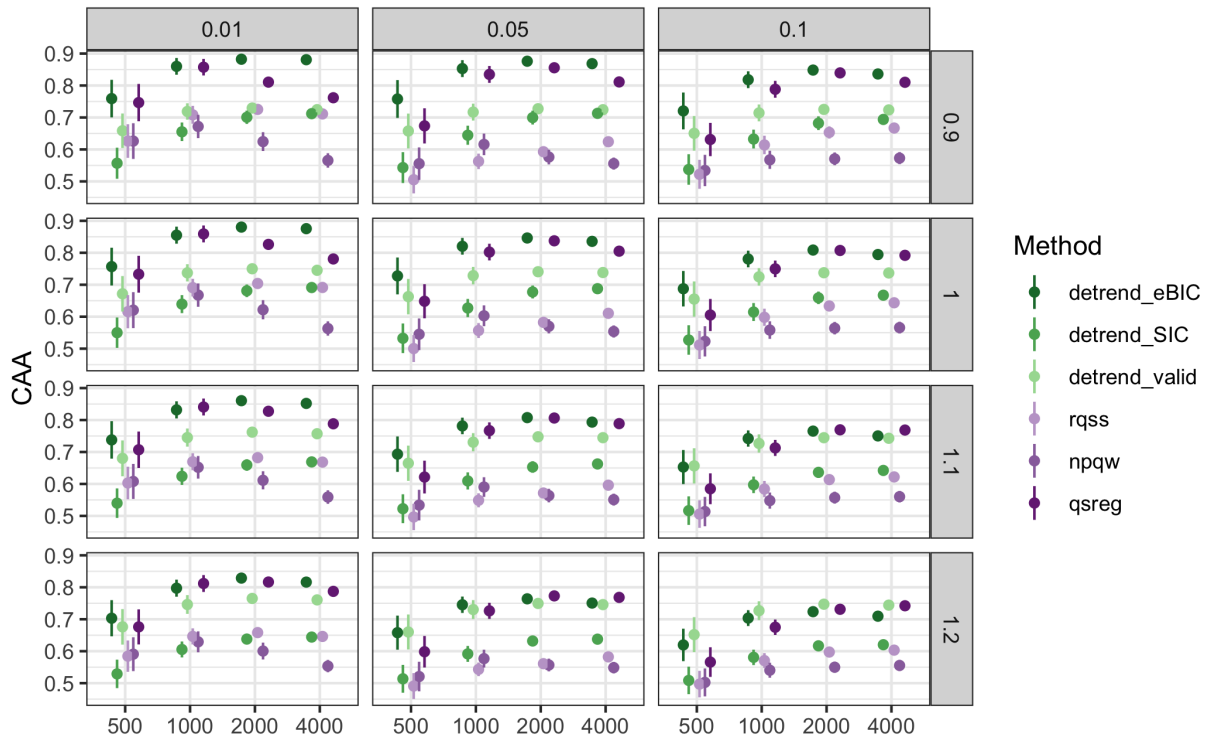

Figure 11: Class averaged accuracy by threshold, data size, and method (1 is best 0.5 is worst).

4 Application

The low-cost "SPod" air quality sensors output a time series that includes a slowly varying baseline, high frequency random noise, and the sensor response to pollutants. A potential use for these sensors is to monitor pollutant concentrations at the fence lines of industrial facilities and detect time points when high concentrations are present. Ideally, three co-located and time aligned sensors (as shown in Figure 2) responding to a pollutant plume would result in the same signal classification after baseline trend removal and proper threshold choice.

We compare our `detrend_eBIC` method with the `qsreg` method on a subset of the SPod data (n=6000) since the `qsreg` method cannot handle all 24 hours simultaneously. We estimate the baseline trend using the 10^{th} and 15^{th} quantiles and compare three thresholds for classifying signal. The thresholds are calculated using the median plus a multiple of

Figure 12: Estimated 15$^{\text{th}}$ quantile trends on subset of the data using `qsreg` and `detrend_eBIC`.

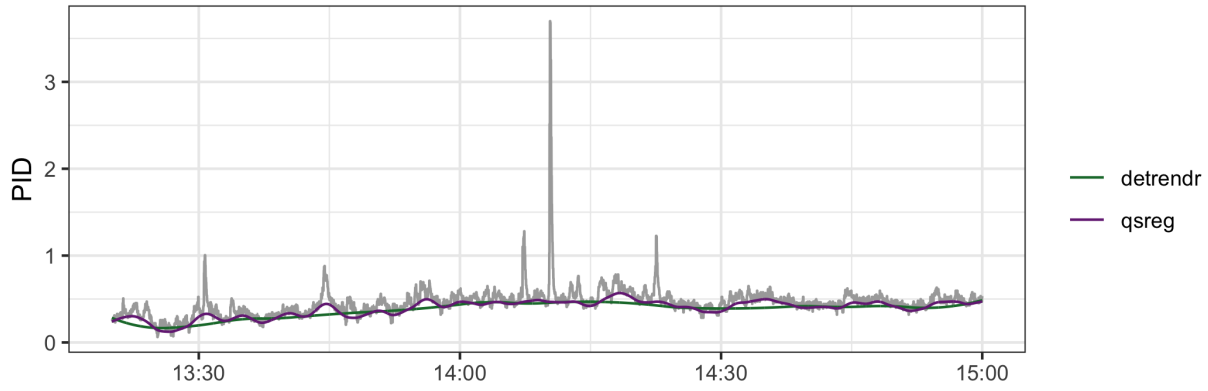

the median absolute deviation (4) of the detrended series.

$$\text{MAD} \quad = \quad \text{median}(y - \tilde{y}), \tag{4}$$

where $\tilde{y}$ is the median of y. Given a method, quantile level, and MAD multiple, we estimate the quantile trend for each of the sensor nodes and subtract it from the observations. We then calculate the threshold using the median plus the MAD multiple of the corrected series and classify the corrected series based on the threshold. An example of the estimated baseline fit for each method is shown in Figure 12, while Figure 13 shows the series after subtracting the `detrend_eBIC` estimate of the 15$^{\text{th}}$ quantile and classifying the signal using a MAD multiple of 3.

Given the signal classifications for node 1, $s_1(t) \in \{0, 1\}$ and node 2, $s_2(t) \in \{0, 1\}$ we want to compare the similarity between the two classifications. One metric for evaluating the distance between two classifications is the variation of information (VI):

$$\begin{aligned} r_{ij} \quad &= \quad \frac{1}{n} \sum_t \mathbb{1}(s_1(t) = i \cap s_2(t) = j) \\ \text{VI}(s_1, s_2) \quad &= \quad -\sum_{i,j} r_{ij} \left[\log \left(\frac{r_{ij}}{\frac{1}{n} \sum_t \mathbb{1}(s_1(t) = i)} \right) + \log \left(\frac{r_{ij}}{\frac{1}{n} \sum_t \mathbb{1}(s_2(t) = j)} \right) \right] \end{aligned}$$

The VI is a distance metric for measuring similarity of classifications and will be 0 if the classifications are identical and increase as the classifications become more different. The

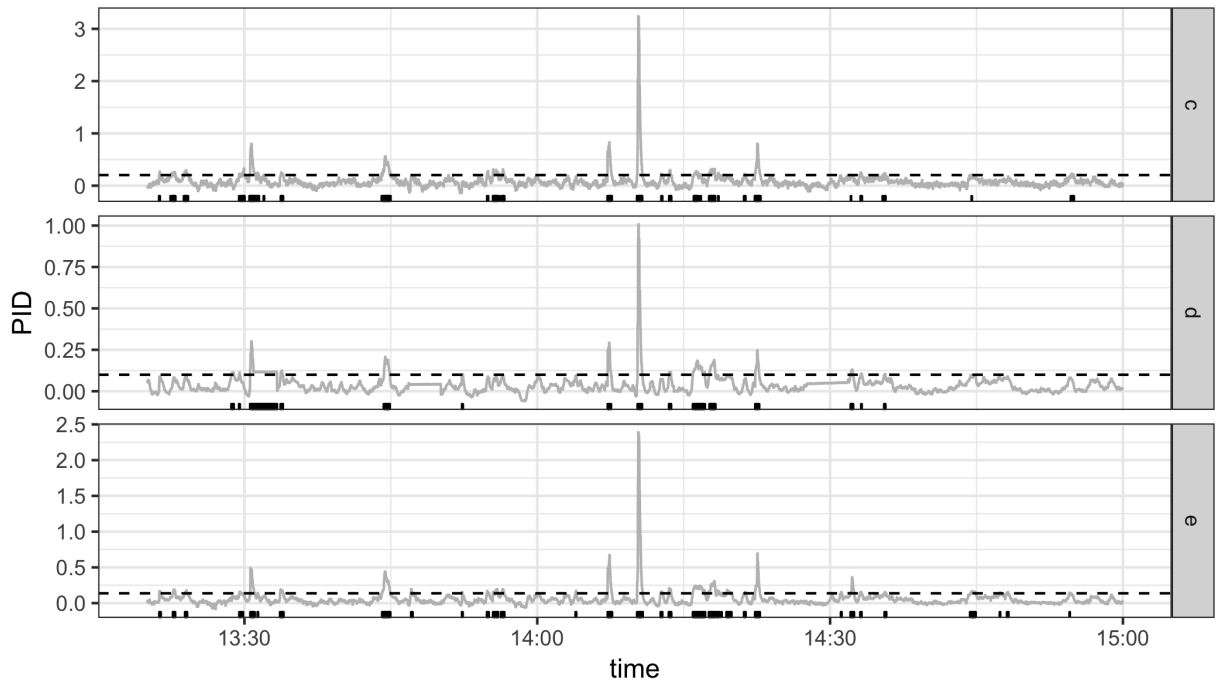

Figure 13: Rugplot showing locations of signal after baseline removal using detrendr estimate of 15th quantile. Horizontal dashed lines represent the thresholds.

VIs by method, quantile and trend are shown in Figure 14. In all cases our `detrend` method results in classifications that are more similar than those from the `qsreg` method. As is illustrated in Figure 12 and Figure 13, our method results in a smoother baseline estimate which improves signal classification.

Our windowed `detrend_eBIC` method was used to removed the baseline drift from the total dataset consisting of 86,401 observations per node. The VI scores for the full dataset were 0.36, 0.24, and 0.41 for nodes c and d, c and e, and d and e, respectively. The complete confusion matrices for the nodes using a MAD multiple of 5 for the threshold is given in Table 1.

5 Conclusion and Discussion

We have expanded the quantile trend filtering method by implementing a non-crossing constraint and a new algorithm for processing large series, and proposing a modified criteria for

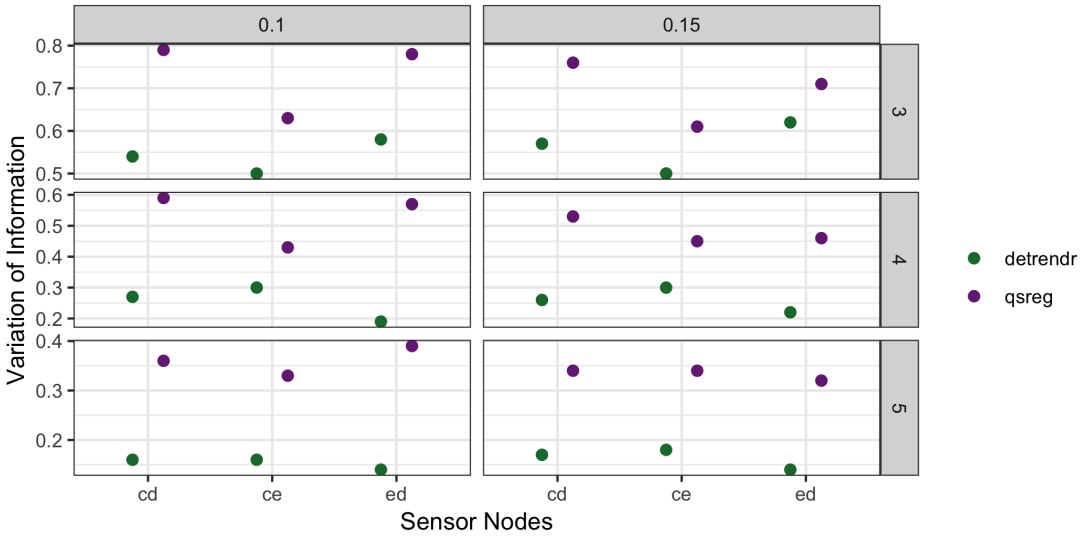

Figure 14: Variation of Information between sensor nodes after trend removal by quantile and method and thresholding by factor of MAD.

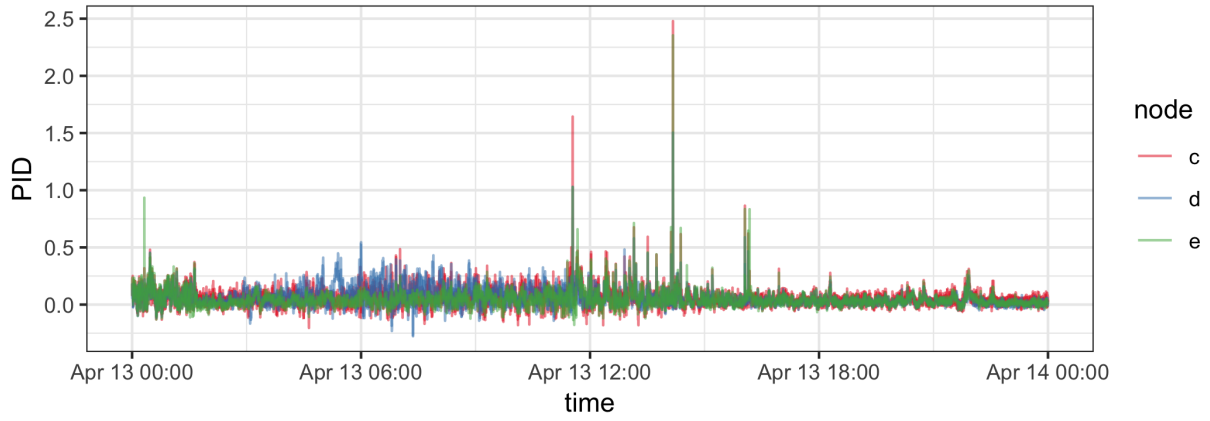

Figure 15: Low cost sensor data after drift removal using windowed detrend with eBIC.

Table 1: Confusion matrices for 3 SPod nodes after baseline removal using 15th quantil and threshold of 3*MAD (n=52322).

	c = 0		**c = 1**	
	e = 0	e = 1	e = 0	e = 1
d = 0	80383	578	2551	145
d = 1	1298	737	111	598

smoothing parameter selection. Furthermore we have demonstrated the utility of quantile trend filtering in both simulations and applied settings. Our ADMM algorithm for large series both reduces the computing time and allows trends to be estimated on series that cannot be estimated simultaneously while our scaled extended BIC criteria was shown to provided better estimated of quantile trends in series with and without a signal component. We have also shown that the baseline drift in lost-cost air quality sensors can be removed through estimating quantile trends.

In the future, quantile trend filtering could be extended to observations measured at non-uniform spacing by incorporating the distance in covariate spacing into the differencing matrix. It could also be extended to estimate smooth spatial trends by a similar adjustment to the differencing matrix based on spatial distances between observations.

SUPPLEMENTARY MATERIAL

R-package for detrend routine: R-package detrendr containing code to perform the diagnostic methods described in the article. (GNU zipped tar file)

References

Boyd, S., Parikh, N., Chu, E., Peleato, B., Eckstein, J., et al. (2011), "Distributed optimization and statistical learning via the alternating direction method of multipliers," *Foundations and Trends® in Machine learning*, 3, 1–122.

Brantley, H., Hagler, G., Kimbrough, E., Williams, R., Mukerjee, S., and Neas, L. (2014), "Mobile air monitoring data-processing strategies and effects on spatial air pollution trends," *Atmospheric measurement techniques*, 7, 2169–2183.

Chen, J. and Chen, Z. (2008), "Extended Bayesian information criteria for model selection with large model spaces," *Biometrika*, 95, 759–771.

Gabay, D. and Mercier, B. (1975), *A dual algorithm for the solution of non linear variational problems via finite element approximation*, Institut de recherche d'informatique et d'automatique.

Glowinski, R. and Marroco, A. (1975), "Sur l'approximation, par éléments finis d'ordre un, et la résolution, par pénalisation-dualité d'une classe de problèmes de Dirichlet non linéaires," *Revue française d'automatique, informatique, recherche opérationnelle. Analyse numérique*, 9, 41–76.

Gurobi Optimization, L. (2018), "Gurobi Optimizer Reference Manual," .

Kim, S.-J., Koh, K., Boyd, S., and Gorinevsky, D. (2009), "ℓ_1 Trend Filtering," *SIAM Review*, 51, 339–360.

Koenker, R. and Bassett, G. (1978), "Regression Quantiles," *Econometrica*, 46, 33–50.

Koenker, R., Ng, P., and Portnoy, S. (1994), "Quantile smoothing splines," *Biometrika*, 81, 673–680.

Marandi, R. Z. and Sabzpoushan, S. (2015), "Qualitative modeling of the decision-making process using electrooculography," *Behavior research methods*, 47, 1404–1412.

Ning, X., Selesnick, I. W., and Duval, L. (2014), "Chromatogram baseline estimation and denoising using sparsity (BEADS)," *Chemometrics and Intelligent Laboratory Systems*, 139, 156 – 167.

Nychka, D., Gray, G., Haaland, P., Martin, D., and O'connell, M. (1995), "A nonparametric regression approach to syringe grading for quality improvement," *Journal of the American Statistical Association*, 90, 1171–1178.

Oh, H.-S., Lee, T. C. M., and Nychka, D. W. (2011), "Fast Nonparametric Quantile Regression With Arbitrary Smoothing Methods," *Journal of Computational and Graphical Statistics*, 20, 510–526.

Pettersson, K., Jagadeesan, S., Lukander, K., Henelius, A., Hæggström, E., and Müller, K. (2013), "Algorithm for automatic analysis of electro-oculographic data," *Biomedical engineering online*, 12, 110.

Racine, J. S. and Li, K. (2017), "Nonparametric conditional quantile estimation: A locally weighted quantile kernel approach," *Journal of Econometrics*, 201, 72–94.

Snyder, E., Watkins, T., Solomon, P., Thoma, E., Williams, R., Hagler, G., Shelow, D., Hindin, D., Kilaru, V., and Preuss, P. (2013), "The changing paradigm of air pollution monitoring." *Environmental science & technology*, 47, 11369.

Theussl, S. and Hornik, K. (2017), *Rglpk: R/GNU Linear Programming Kit Interface*, r package version 0.6-3.

Thoma, E. D., Brantley, H. L., Oliver, K. D., Whitaker, D. A., Mukerjee, S., Mitchell, B., Wu, T., Squier, B., Escobar, E., Cousett, T. A., et al. (2016), "South Philadelphia passive sampler and sensor study," *Journal of the Air & Waste Management Association*, 66, 959–970.

Tibshirani, R. J. (2014), "Adaptive piecewise polynomial estimation via trend filtering," *The Annals of Statistics*, 42, 285–323.

Yamada, H. (2017), "Estimating the trend in US real GDP using the 1 trend filtering," *Applied Economics Letters*, 24, 713–716.

Yu, K. and Moyeed, R. A. (2001), "Bayesian quantile regression," *Statistics & Probability Letters*, 54, 437–447.